Journal of the European Ceramic Society 17 (1997) 813–818

PII: S0955-2219(96)00133-1
0955-2219/97/$17.00

PZT Phase Formation Monitored by High-Temperature X-Ray Diffractometry

Oleg Babushkin,[a] Ture Lindbäck,[a] Keith Brooks[b] & Nava Setter[b]

[a]Luleå University of Technology, Division of Engineering Materials, S-971 87, Luleå, Sweden
[b]Laboratoire de Céramique, Ecole Polytechnique Federale de Lausanne, Lausanne, Switzerland

(Received 8 February 1996; accepted 23 July 1996)

Abstract

The crystallisation kinetics of amorphous sol–gel PZT thin films were investigated using high-temperature X-ray diffraction. Crystallisation for different isotherms was monitored as a function of time. Phase transformation data were obtained from integrated X-ray peak intensities which were calibrated based on image analysis of the surface microstructure of the samples at the end of the isothermal treatments. An activation energy of 310 kJ/mol was obtained without assuming a specific kinetic model. From the transformation data, a TTT diagram was constructed for the ranges studied. © *1997 Elsevier Science Limited. All rights reserved.*

1 Introduction

The technological importance of $Pb(Zr_{1-x}Ti_x)O_3$ (PZT) thin films is evidenced in their use in ferroelectric memory applications and micro-electromechanical systems. Sol–gel has been one of the most reported methods for the preparation of PZT films, yet little is known about the kinetics of the transformation from as-deposited amorphous 'gels' to fully crystalline films of perovskite structure. Knowledge of the mechanisms of nucleation and growth of sol–gel PZT films is important for a determination of which parameters most strongly influence the final grain size and microstructure. For ferroelectric memory applications, films of columnar microstructures[1] and lateral grain sizes of the order of the film thickness are sought in order to obtain optimum switching characteristics.

Voight *et al.*[2] investigated the crystallisation of PZT 20/80 sol–gel thin films treated isothermally in the temperature range of 475 to 525°C by rapid thermal annealing and reported an activation energy of 326 kJ/mol. Films were <100>/<001> oriented grown on single crystal MgO. Crystallisation kinetics of sputter-deposited $Pb(Zr_{0.55}Ti_{0.45})O_3$ films annealed in the temperature range of 525 to 574°C were reported by Kwok, with activation energies of the order of 494 kJ/mol.[3] Hu *et al.* reported on the qualitative effect of heating rates on the phase transformations which occur during the annealing of sputtered PZT films of composition $Pb(Zr_{0.50}Ti_{0.50})O_3$.[4] It was concluded that the crystallisation path changes from a direct amorphous to perovskite conversion for fast heating (RTA) to an amorphous-pyrochlore-perovskite reaction sequence for slow (conventional) annealing. The kinetics of formation of $PbTiO_3$ powders from metallo-organic precursors has been reported by Shaikh and activation energy values in the range of 60 to 87 kJ/mol were obtained.[5]

In this investigation, isothermal high-temperature X-ray diffraction was used to investigate the transformation kinetics of amorphous PZT thin films prepared using a sol–gel method.

2 Experimental

2.1 PZT film preparation

Silicon substrates with SiO_2, Ti and Pt layers of 1 μm, 1 nm and 10 nm thickness, respectively, were used in this study. Amorphous sol–gel-derived PZT films were deposited by spin coating thin layers of approximately 50 nm thickness, followed by pyrolysis at 350°C and repetition of the process to achieve films of 0·5 μm thickness (before annealing). Preparation of the sol–gel precursor follows the procedure of Budd[6] and is described in more detail in a previous paper.[7] After deposition, films were crystallised directly in an X-ray diffractometer equipped with a hot stage.

2.2 High-temperature XRD

In-situ X-ray diffraction investigations were performed using an automated diffractometer (Philips PW-1710) equipped with a high-temperature attachment engineered by the authors. The high-temperature

chamber was constructed explicitly for isothermal thin film crystallisation studies. Thus a furnace capable of rapid heating was designed. Continuous scanning was performed with Cu K_a (50 kV, 30 mA) radiation and a graphite monochromator. Diffractograms were collected from 20–50° 2θ for all samples. In order to follow the crystallisation of the PZT and pyrochlore phases, data for the (100), and (110) PZT peaks and the (222) pyrochlore peak were obtained using two subscans within the ranges 21·6 to 22·8 and 27·5 to 32° 2θ. The temperature of the sample was measured with a Pt-13/Rh/Pt thermocouple. In all cases, the heating rate used to attain the temperature of interest was 5°C/s. In-situ investigations of phase development were performed during isothermal heat treatment in the temperature range 620–670°C with a 60-min maximum soaking time. The quantitative phase analysis involved a precise measurement of the integrated intensities of the perovskite (100), and (110) peaks and pyrochlore (222) peak. The profile fitting technique used was based on a Marguardt non-linear least squares algorithm.

2.3 Microstructural characterisation by SEM

The percentage conversion to perovskite and the quantity of residual pyrochlore were determined for each isothermal treatment using a combination of scanning electron microscopy (JEOL 6300, Japan) and quantitative image analysis. Templates for the image analysis were prepared by tracings from the SEM photomicrographs.

3 Results and Discussion

3.1 Microstructural analysis

A field emission scanning electron microscope (5 kV accelerating voltage) was used to characterise the microstructure of the film surfaces at the end of each of the isothermal treatments. Image analysis was then used to calculate the volume percentage conversion to perovskite phase and the quantity of residual pyrochlore phase. For the image analysis, it was assumed that the grains are columnar in nature, based on previous studies, such that the fraction of surface area attributed to perovskite is equivalent to the volume fraction of PZT.[7,8] Typical micrographs for the different isotherms are shown in Fig. 1. The average values of perovskite content are presented in Table 1.

3.2 XRD analysis

Examination of diffraction patterns of the thin films before crystallisation revealed the presence of a wide and diffused 'halo' in the range of 22 to 35° 2θ which originates from scattering by an amorphous phase (Fig. 2). The location of the centroid of this 'halo', within approximately 28 to 29 2θ indicates the existence of structural units similar to those in stoichiometric perovskite or pyrochlore PZT. Previous TEM and XRD investigations have shown similar results.[7,8] Subsequent isothermal treatments in the range 620–670°C initiated transformation of the amorphous phase to the crystalline perovskite structured PZT phase.

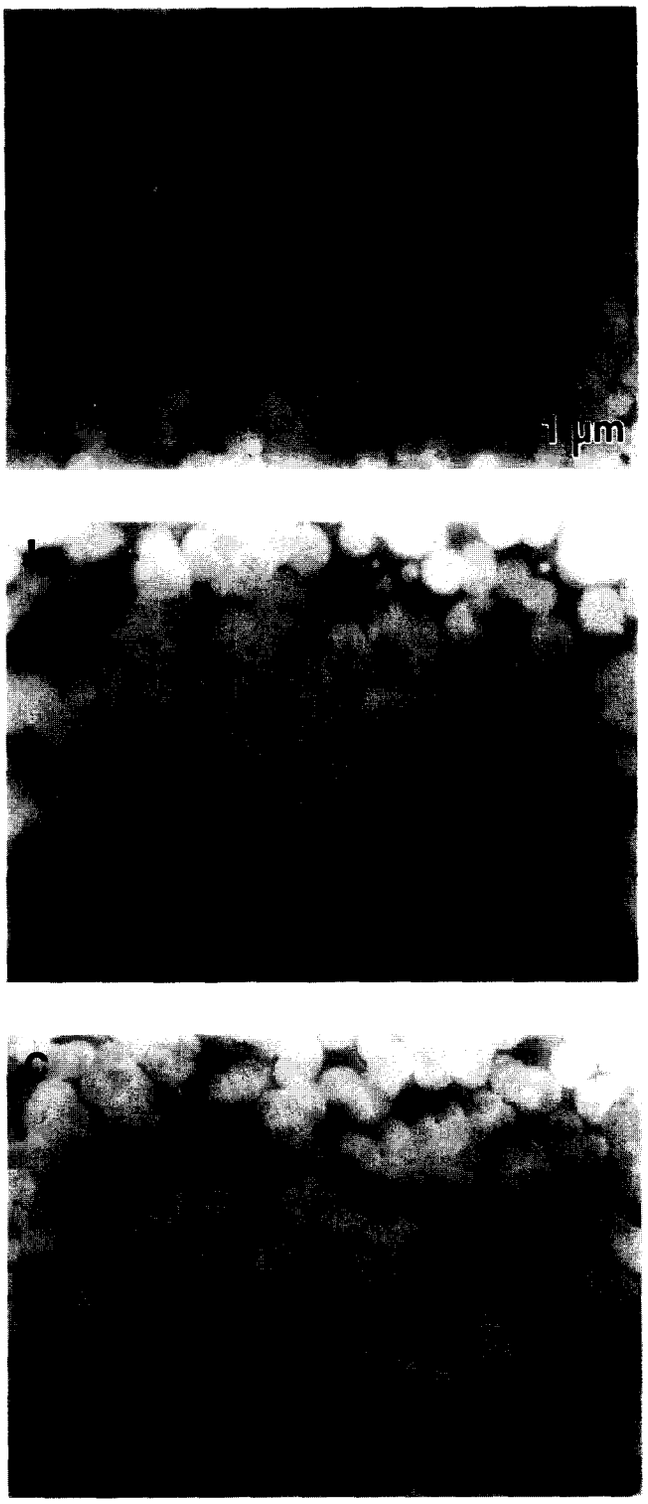

Fig. 1. SEM Photomicrographs showing the surfaces of the films after isothermal annealing at (a) 620, (b) 640 and (c) 670°C.

Traces of $Pb_2Ti_2O_7$ pyrochlore phase were observed as well (Fig. 2).

Marguardt non-linear least squares fitting was applied for profile analysis of the (100), and (110) perovskite peaks and the (222) pyrochlore peak. Examples of the fitted profiles are illustrated in Fig. 3. The 100 peak is of highest intensity indicating a strong (100) texture. PZT films of analogous texture prepared on Ti/Pt bilayer metallisations on Si have been reported previously.[8] The diffused (222) pyrochlore peak which appears in the X-ray scans exhibits the same profile over the complete range of times and temperatures investigated. The intensity of this peak changes with time for a given isothermal treatment, yet the width remains constant. The constant width of the (222) peak throughout the transformation process indicates that no growth of the pyrochlore crystallites occurs, being maintained as nano-crystallites throughout the perovskite transformation process.

Table 1. Summary of image analysis data

Temperature (°C)	*Area of micrograph* (μm^2)	*Perovskite conversion* (%)
620	400	46·41
640	400	67·53
670	400	71·64

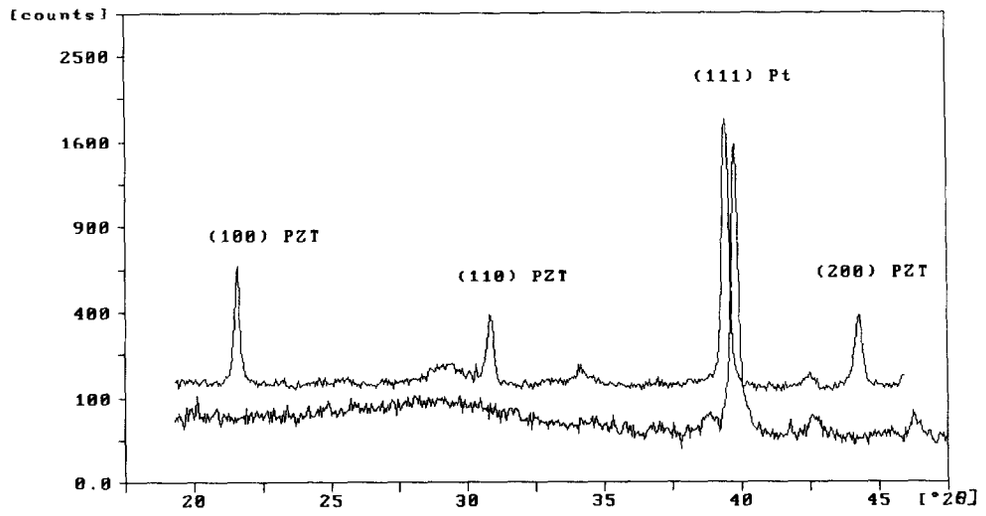

Fig. 2. Diffraction patterns of the PZT thin film before and after heat treatment at 670°C.

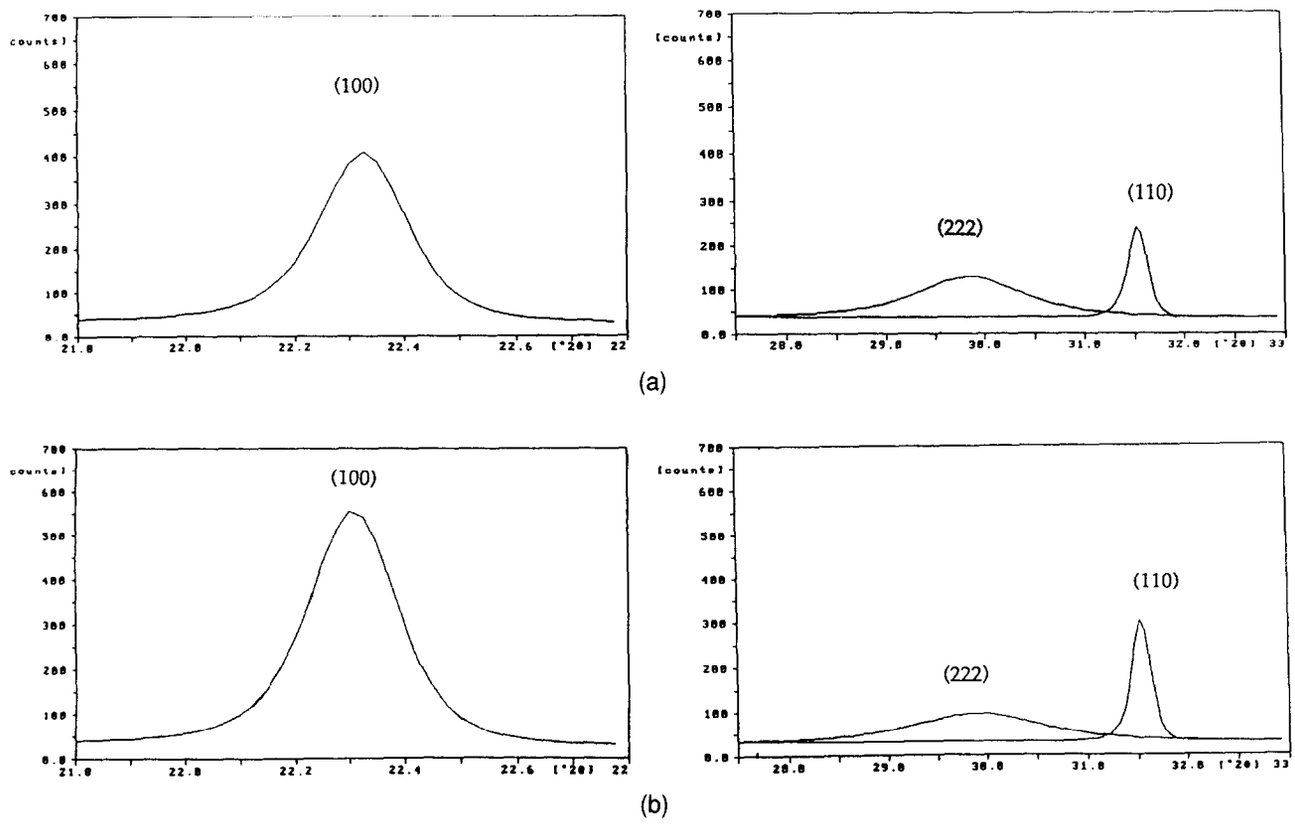

Fig. 3. Deconvoluted profiles of (100) and (110) perovskite and (222) pyrochlore phases peaks after treatment at 670°C for soaking times of (a) 5 and (b) 15 min.

The quantitative phase development was estimated by calculation of the integrated intensity of the profile. The use of a maximum profile intensity technique was rejected because of decreased sensitivity in the case of diffuse and broad profiles. The area of the (100) profile was computed within 1° θ, and the areas of the (110) and (222) peaks were computed within 5·5° θ utilising the deconvolution technique noted above. A summary of the integrated intensities of the (110) perovskite and (222) pyrochlore peaks as a function of isothermal soaking time is presented in Fig. 4.

The image analysis method described above was used to quantify the amount of perovskite phase formed at equilibrium at the end of the isothermal treatments. These values were then used to calibrate the XRD data from the computed integrated intensities of the perovskite (100) peak. Good linear proportionality between image analysis and XRD was found. It can be seen that the character of the curves presented (Fig. 5) indicates the existence of an incubation time for crystallisation of the PZT phase which is quite pronounced at 620°C and negligible at 670°C. The resulting curves of fraction transformation were used for the kinetic analysis. A TTT diagram (Fig. 6), which maps the perovskite phase transformation as a function of time and temperature, was constructed from the X-ray data after calibration against image analysis measurement.

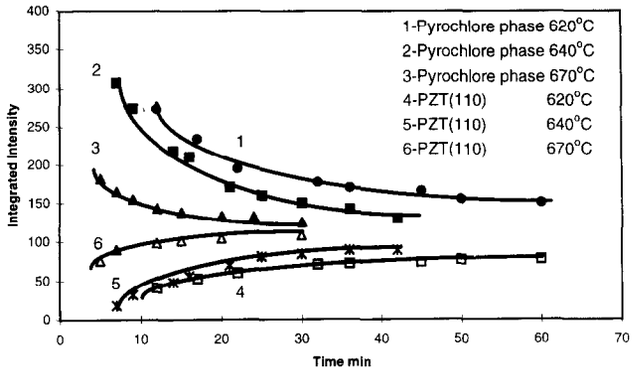

Fig. 4. Integrated intensities of the (222) pyrochlore and (110) PZT peaks versus time.

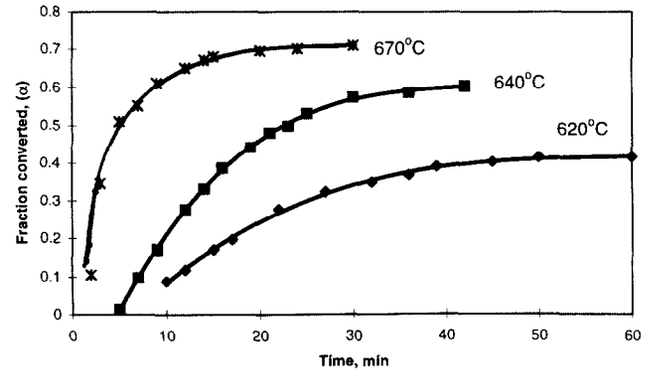

Fig. 5. Fraction of PZT phase formed at different temperatures as a function of annealing time.

3.3 Computation of the activation energy of crystallisation

The overall rate of a microscopic transformation which proceeds via a large number of atomic processes is exponentially related to the reciprocal of the absolute temperature and the activation enthalpy and can be expressed by:[9]

$$\text{rate} = v \exp(\Delta S/k) \exp(-\Delta H/kT) \qquad (1)$$

In condensed matter systems the activation enthalpy, ΔH, and the activation energy, E, are nearly the same. Therefore, the rate of the transformation may be expressed as an exponential function of an empirical activation energy, E, which is characteristic of the transformation process:

$$d\alpha/dt = f(\alpha)^* A \exp(-E/RT) \qquad (2)$$

The rate of the transformation is also expected to depend upon the extent of the transformation (α). Integration of (2) and rearrangement of terms gives:

$$\ln t_{\alpha 1} = \ln\{\int [A\, f(\alpha)]^{-1} d\alpha\} + E/RT \qquad (3)$$

where $t_{\alpha 1}$ is the time required to obtain a certain volume fraction conversion, α. Application of simplified dependence of equal fraction transformed in time reverse temperature helps to reveal the interval of phase transition proceeding with the same rate. As can be seen in Fig. 7, in selected interval the derived plots are reasonably straight and parallel to each other, indicating that the PZT formation is characterised by a uniform mechanism, in the temperature interval investigated.

Evaluation of the activation energy was performed by application of the Avrami equation

$$\alpha = 1 - \exp(-kt)^n \qquad (4)$$

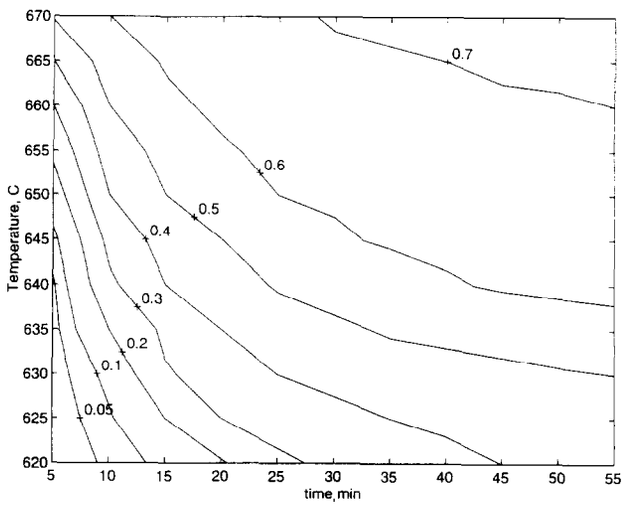

Fig. 6. Time-temperature-transformation (TTT) diagram constructed from the isothermal data. The fractions of transformation indicated on the contour were obtained from the X-ray intensities by calibration against image analysis measurements (see text).

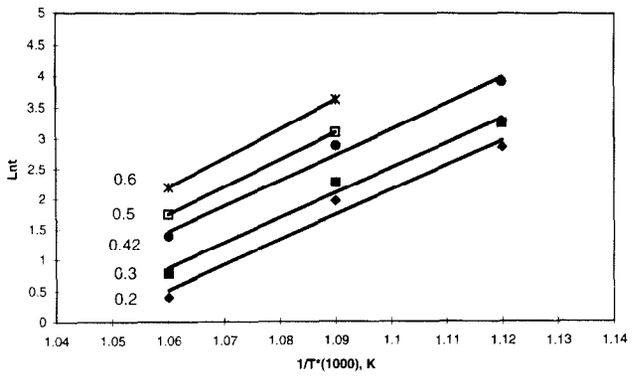

Fig. 7. The logarithm of time as a function of reciprocal temperature for various extent of conversion to perovskite.

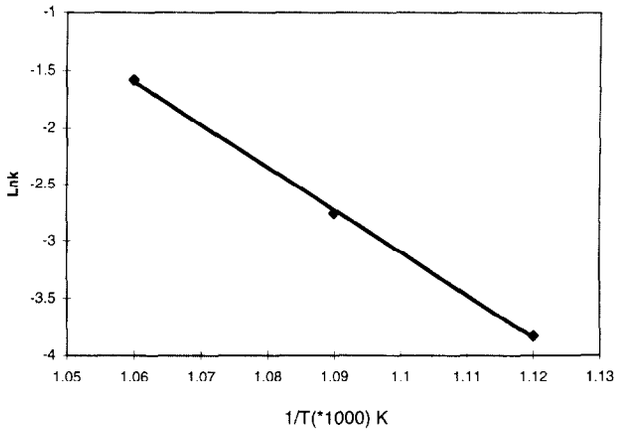

Fig. 9. The dependence of rate constant k versus temperature.

Where α is the volume fraction of the product phase, k is the rate constant and n is a constant whose value depends on the nucleation and growth process. According to this equation, a plot of $\ln\ln[1/(1-\alpha)]$ versus $\ln t$ should yield straight lines with slopes equal to the exponent n and from which the value of k can be derived. Such plots for the present results compared with those of Kwok and Desu[3] are shown in Fig. 8. From the dependence of the rate constant on reciprocal temperature, the activation energy was calculated to be 310 kJ/mole (Fig. 9). This falls within the range of values (275–494 kJ/mol) reported in the literature.[2,3,11] Although the values of activation energy are similar, the reported values of the exponent n in the Avrami equation vary significantly between 1·8 and 2·5.[2,3,11] In this work a value of 0·75 was obtained. Within the framework of a proposed classification of diffusion-controlled transformations,[9] an exponent n greater than 2 indicates that the transformation is nucleation limited, and thus the estimated activation energy can be related to a nucleation energy. In contrast, values of n less than 1 indicate that the crystal growth dominates. Indeed, inspection of the available literature data[2,3,11] indicates that the data used for determination of the rate constant k are strongly dominated by data from low degree of transformation, mainly less than 1% and never higher than 50%. At such low fractions of transformation the process could well be determined by nucleation rather than growth. In this study, the HT-XRD technique has proved to be very effective for ranges beyond the nucleation and early grain growth stages. Thus, the data obtained for the range of transformed fraction from 20 to 60% (Fig. 8), reflect mostly the crystal growth process.

It is of interest to be able to isolate the kinetics of the crystal growth regime from the nucleation regime because the compositional homogeneity through the film thickness can be strongly influenced by the growth mechanism. It has been previously observed[12] that during bottom electrode nucleated crystallisation of sol–gel PZT, Zr preferentially diffuses towards the film surface as crystallisation proceeds. This diffusion in turn slows the growth (increases the growth activation energy) because the activation energy of Zr-rich PZT is greater than that of $PbTiO_3$, and the increased Zr concentration at the growth front increases the stability of the metastable pyrochlore phase. This can lead to the occurrence of residual

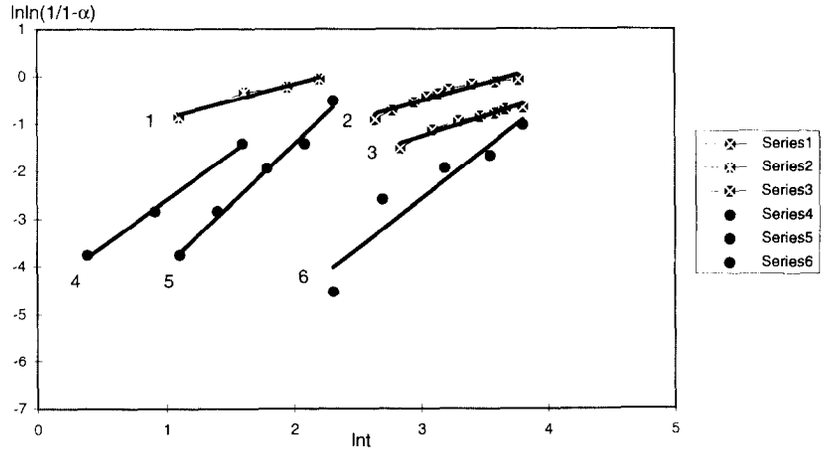

Fig. 8. Plot of $\ln\ln[1/(1-\alpha)]$ versus $\ln t$. Series 1–3 presents data for temperatures 670, 640, and 620°C, series 4–6 from Kwok and Desu[3] for temperatures 575, 550 and 525°C.

pyrochlore on the film surface, and strongly degrade the film properties.

4 Conclusions

The phase transformation of amorphous sol–gel to perovskite was investigated at temperature under isothermal conditions using high-temperature X-ray diffraction. The activation energy for the crystallisation process, determined from quantitative transformation data without assuming a particular physical process, was found to be 310 kJ/mol and was mostly attributed to the grain growth of the perovskite phase.

Acknowledgement

This work was carried out as part of the European COST 514 action entitled: Ferroelectric Ceramic Thin Films.

References

1. Larsen, P. K., Ultrafast polarisation switching of lead zirconate titanate thin films. *Proc. ISAF '92*, 31 Aug.–2 Sept. 1992, pp. 217–224.
2. Voigt, J., Tuttle, B., Headley, T., Eatough, M., Lamppa, D. & Goodnow, D., Oriented lead zirconate titanate thin films: Characterization of film crystallisation, *Mat. Res. Soc. Symp. Proc.*, **310** (1993) 15–21.
3. Kwok, C. & Desu, S., Pyrochlore–perovskite phase transformation of lead zirconate titanate (PZT) thin film. In *Ferroelectric Films, Ceram. Trans. 25*, Am. Ceram. Soc., Westerville, OH, 1992, 85–96.
4. Hu, H., Peng, C. & Krupanidhi, S., Effect of heating rate on the crystallisation behaviour of amorphous PZT thin films. *Thin Solid Films*, **223** (1993) 327–333.
5. Shaikh, A. & Vest, G., Kinetics of $BaTiO_3$ and $PbTiO_3$ formation from metallo-organic precursors. *J. Am. Ceram. Soc.*, **57**(9) (1986) 682.
6. Budd, K. D., Dey, S. K. & Payne, D. A., Sol–gel processing of PT, PZ, PZT and PLZT thin films. *Br. Ceram. Proc.*, **36** (1985) 107–121.
7. Reaney, I. M., Brooks, K., Klissurska, R., Pawlaczyk, Cz. & Setter, N., Use of TEM for the quality assessment of rapid thermally annealed, solution-gel, lead zirconate titanate thin films in argon and oxygen atmospheres. *J. Am. Ceram. Soc.*, **77**(5) (1994) 1209–1216.
8. Brooks, K. G., Reaney, I. M., Klissurska, R., Huang, Y., Bursill, L. & Setter, N., Orientation of rapid thermally annealed, solution-gel, lead zirconate titanate films. *J. Mat. Res.*, **9**(10) (1994) 2540–2553.
9. Rao, C. & Rao, K., *Phase Transformation in Solids*. W & J Mackay Ltd, Chatham, UK, 1978.
10. Porter, D. & Easterling K., *Phase Transformations in Metals and Alloys*. T. Press Ltd, Cornwall, UK, 1988.
11. Griswold, E. M., Weaver, L., Calder, I. D. & Sayer, M., Rapid thermal processing and crystallisation kinetics in lead zirconate (PZT) thin film. *Mat. Res. Soc. Symp. Proc.*, **361** (1995) 389–394.
12. Klissurska, R. D., Brooks, K. G., Reaney, I. M., Pawlaczyk, Cz., Kosec, M. & Setter, N., Effect of Nb doping on the microstructure of sol–gel derived PZT thin films. *J. Am. Ceram. Soc.*, **78**(6) (1995) 1513–1520.